

# Sedimentation processes and history under the northern Iberian upwelling system

I.R. Hall<sup>1</sup>, I.N. McCave<sup>1</sup> and R. Bao<sup>2</sup>

<sup>1</sup>Department of Earth Sciences, University of Cambridge, United Kingdom

<sup>2</sup>Área de Xeoloxía Universidade da Coruña, Spain

## 1. INTRODUCTION

The contribution of the University of Cambridge to OMEX II-II is as follows:

80% Work Package III Fluxes and Processes in the Nepheloid Layers and Surface Sediments

20% Work Package IV Integrated Margin-Exchange Product.

1. determine SPM concentration and composition (**Task III.1.1**)
2. make particle accumulation and mixing rate determinations in box-core sediments (**Task III.1.3**)
3. measure sediment grain-size, diatom contents and <sup>13</sup>C isotope determination of organic carbon (**Task III.1.4**)
4. make comparison with results OMEX I at Goban Spur (**Task III.1.5**)
5. determine down-core variability of sediment composition and properties in long (Kasten) cores and estimate eolian influence (**Task III.1.7**)
6. make organic carbon determinations and C/N ratios for estimation of carbon burial fluxes
7. estimate total SPM and POC as particulate components in the pelagic cycling of carbon (**Task IV.2**) and of particle fluxes and budgets
8. analyse cores for the long-term record of benthic cycling and burial carbon (**Task IV.5**)
9. responsible for estimating the sensitivity of upwelling systems to environmental change
10. analyse cores for indicators of past upwelling cycles and distributions, and run model scenarios for varied climate forcing, to estimate sensitivity to climate change (**Task IV.5**)

This report provides an overview of the first two years work carried out in the Department of Earth Sciences at Cambridge in support of the OMEX II-II objectives as outlined above.

## 2. PARTICULATE MATTER DISTRIBUTION (ITEMS 1 AND 4)

We have collected a total of 94 CTD stations providing detailed hydrographic data on temperature, salinity, oxygen, fluorescence, transmission and scattering obtained during two cruises: *Charles Darwin CD105* (29 May - 22 June 1997) and *CD110* (23 Dec 1997 - 19 Jan 1998) providing moderate temporal coverage. Details of the station positions, methods and the empirical calibration of both the transmissiometer and Light Scattering Sensor are given in the first annual report.

The general features of the fence diagram (Fig. 1; produced by Rudnicki's (1977) program) show a subsurface peak in particle load associated with the chlorophyll maximum at the nutri-and pycnocline at about 50-60 m depth (15-16°C) which decreases in intensity offshore. Strong intermediate nepheloid layers are seen in North Atlantic Central Water (NACW), underlain by relatively clear Mediterranean Water. North Atlantic Deep Water (NADW) is mostly represented by low particle concentrations typical of clear water (~8-15 µg l<sup>-1</sup>), although some higher turbidity Intermediate Nepheloid Layers (INLs) are observed. Only very dilute nepheloid layers are found, particularly at deep stations suggesting weak off-shelf transport of material and weak bottom current resuspension. While, high turbidity close to the shelf break is a feature of a number of sections, the fence diagram highlights, in particular, the presence of an extensive high turbidity plume of near surface water (~15-20 m depth) along section 'Q'. This section is located within a slope embayment off the Ria de Arosa and the high turbidity, with PMCs near the surface in excess of 400 µg l<sup>-1</sup> (estimated from beam attenuation), is associated with lower salinity water present in the upper 25 m that is not seen in any of the other transects.

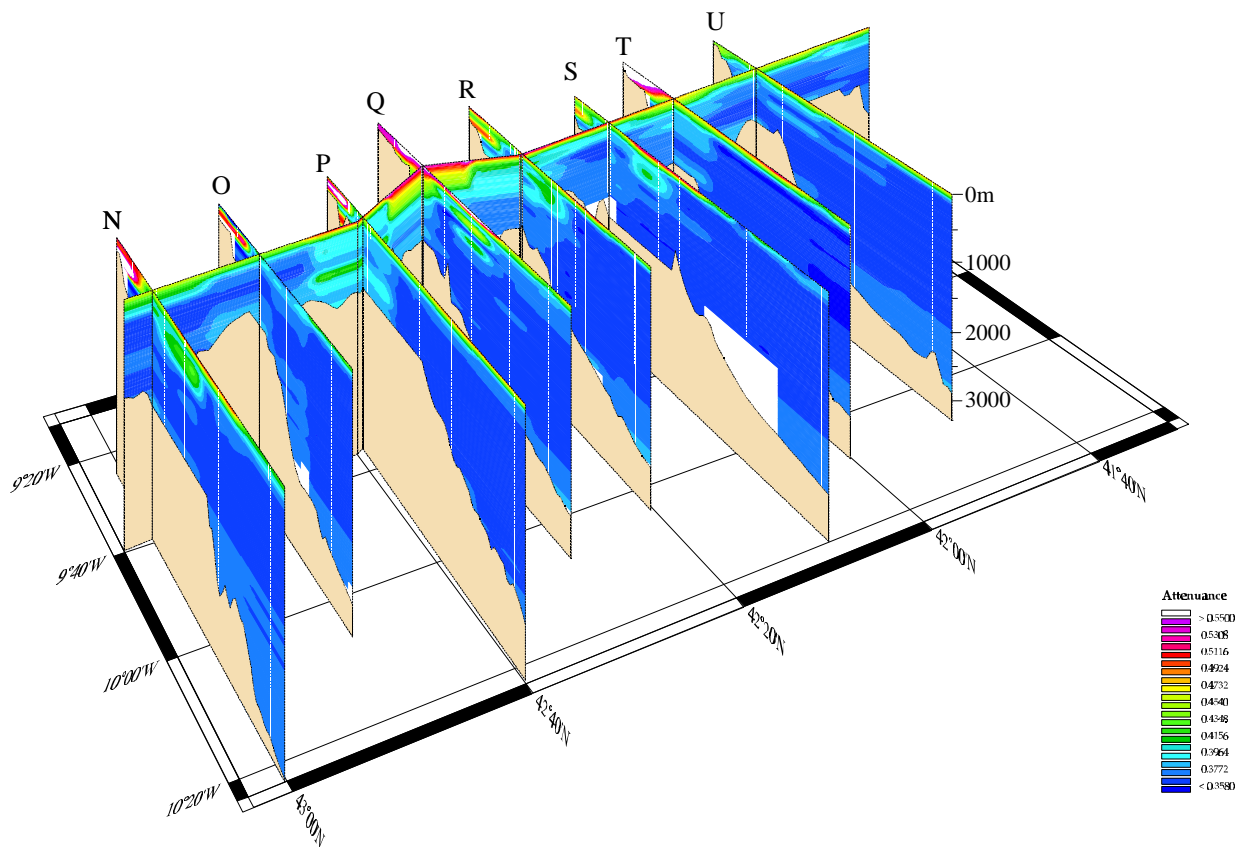


Fig. 1: Fence diagram of beam attenuation in across shelf sections on the Iberian Margin during June 1997 (cruise *CD105*). The bathymetry is the linear track between station positions, transect V is not included in this plot as seabeam bathymetry did not cover this area.

### 2.1. Intermediate nepheloid layers

High concentration INLs are mainly seen in NACW and appear to have a degree of both along and off slope continuity (Fig. 2). Lower concentration INLs are also seen off slope in NADW. The two types of INL differ in scattering and attenuation response. The deep layers show excess scattering suggesting freshly eroded fines, but the shallow layers have about equal response suggesting a greater component of larger, possibly organic-rich, particles resuspended from the upper slope. Intermediate nepheloid layer generation requires an increase of current speed to the critical erosion velocity of 15-20  $\text{cm s}^{-1}$  (McCave, 1984; Gross and Williams, 1991).

The structure, intensity and depth of the shallow INLs seen during this work are similar to those described for the continental slope west of the Porcupine Bank by Dickson and McCave (1986) and the deeper ones resemble those recorded by Thorpe and White (1988). Dickson and McCave (1986) inferred that near bottom water movements were enhanced during periods of particular wind forcing. In their model the mechanism for the intensification resulted from a critical match between the  $M_2$  internal tidal component characteristic and the topographic slope. They suggest such a match arose through changes in the near bottom density gradient during periods of long slope northerly winds producing upwelling. Under such conditions the net Ekman off-slope transport raised the  $\sigma_t \approx 27.3$ - $27.4 \text{ kg m}^{-3}$  density surfaces from a position against the slope to one overlying the break in the slope of the Porcupine Bank at 400-500 m. Once in the water column, these resuspended sediments within the BNL appear to be laterally advected along and off-slope along isopycnals. While in the present study CTD casts are not at a sufficient density, over the shelf break region, to resolve this process, the general conditions were favourable for such a generation mechanism of enhanced near bottom flow to have been present during *CD105*, with dominantly along slope northerly winds during the cruise. It is interesting to speculate that during the summer months when the Azores high-pressure cell, in the central North Atlantic, drives trade winds with southerly components along the coast of Northern Iberia. The resulting equatorward slope current and offshore upwelling of NACW may favour more intense INL production.

Good agreement between particulate matter concentration estimated from the empirical calibration of beam attenuation and scattering is found in clear water, while differences in instrumental response within the benthic and surface nepheloid layers are most likely related to the differing nature of the particles present. In the upper ocean particle load calculated from beam attenuation shows a considerable excess over that calculated by scattering. Offshore spatial and temporal differences in the relationship between both measurements are consistent with a response to large particle sized biological material present in the surface layer.

## 2.2. Particulate organic carbon and nitrogen

Particulate organic carbon (POC) concentration at 10 m ranges between 1.8 and 11.2  $\mu\text{mol l}^{-1}$  decreasing off shelf and towards the south. There is a distinct plume with elevated POC values extending offshore between  $\sim 42$  and  $42.6^\circ\text{N}$ . This feature is coincident with the near surface elevated PMC and low-salinity plume seen in Fig. 1. Carbon: nitrogen ratios of particulate matter at 10 m range from 4.9 to 9.2 and show generally a north-south decreasing trend with the lowest values being seen on the shelf stations close to the Ria de Vigo. Elevated C/N ratios are seen on the Q-transect associated with the high turbidity-low salinity plume, possibly indicating a higher proportion of partially degraded resuspended material present in the water column. Vertical profiles of POC, PON and C/N show only minor variation between stations in the southern transects and a greater degree of variability towards the north. As observed in the 10-m samples there is a clear trend towards higher C/N ratios towards the north.

The PMC estimated by beam attenuation at 10 m shows a strong positive relationship with POC whereas the relationship between LSS-particle load and POC is flatter and less significant (Fig. 2) showing that scattering is relatively insensitive to the surface (fresh) biological material. However, the excess of beam attenuation over LSS-particle load has an equally strong relationship to POC as the beam attenuation and we suggest may be considered as an index of large organic particles (see also Bishop, 1999).

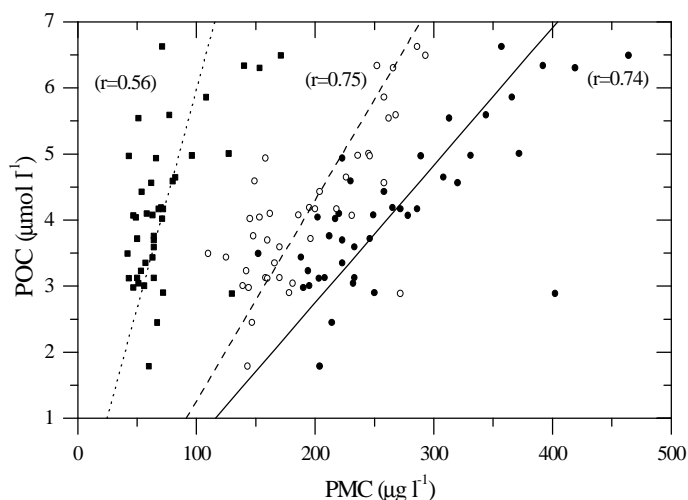


Fig. 2: POC concentration *versus* PMC determined by beam attenuation ( $\text{PMC}^c$ ; filled circles), scattering ( $\text{PMC}^v$ ; filled squares) and beam attenuation excess ( $\text{PMC}^c - \text{PMC}^v$ ; open circles) at 10 m during *CD105*.

The regression of the PMC ( $\mu\text{g l}^{-1}$ ) estimated by beam attenuation *versus* POC ( $\mu\text{g l}^{-1}$ ) (Fig. 2): the POC:PMC ratio, has a value of 0.25 similar to the ratio of total sinking material and organic carbon flux seen in sediment traps ( $\sim 0.25-0.125$ ; Martin *et al.*, 1993). The ratio for beam attenuation excess is 0.37 and is (perhaps only fortuitously), identical to that found during bloom conditions of the North Atlantic Bloom Experiment (Gardner *et al.*, 1993). This suggests that particulate matter in the upper water column during pre-upwelling conditions is dominated by organic components of biological origin.

### 2.3. Particulate matter distribution and $^{234}\text{Th}/^{238}\text{U}$ disequilibrium along the Northern Iberian Margin: implications for particulate organic carbon export

[See also report of Partner 27 (Schmidt, S. and, Reyss, J.L. Laboratoire des Sciences du Climat et de l'Environnement LSCE)].

The upper ocean  $^{234}\text{Th}$  activity was measured at a total of 23 stations occupied during the summer cruise. The broadly uniform distribution of total  $^{234}\text{Th}$  ( $^{234}\text{Th}^{\text{t}}$ ), and more variable particulate  $^{234}\text{Th}$ , suggests that during pre-upwelling conditions on the Iberian Margin,  $^{234}\text{Th}$  distribution is strongly influenced by particle type. As a consequence, particle residence times derived from  $^{234}\text{Th}/^{238}\text{U}$  disequilibria show a considerable range between 4 and 193 days.

#### 2.3.1. Influence of particles on $^{234}\text{Th}$ scavenging

Particle residence times ( $\tau^{\text{p}}$ ) derived from  $^{234}\text{Th}$  deficit show large meso-scale spatial variability, while there is no notable difference in the  $^{234}\text{Th}^{\text{t}}$  activities over the studied area. The basic assumption is that particle concentration, irrespective of composition, plays a major role in scavenging of  $^{234}\text{Th}$  in the upper waters (Santschi and Honeyman, 1991). Possible differences in scavenging rates among different classes of particles, such as phytoplankton, detrital particles and colloids, have been noted (Niven *et al.*, 1995; Baskaran *et al.*, 1996).

As shown above, the near surface particle concentration, as measured by both beam attenuation and scattering, decreases offshore. For the deeper stations, the integrated particle load estimated by beam attenuation over the upper 50 m water depth shows a weak but nevertheless significant ( $r=0.51$ ,  $n=13$ ,  $0.05 < P < 0.1$ , excluding station V2200) correlation with particle residence time. As expected, this shows particle concentration plays a major role in scavenging of  $^{234}\text{Th}$ . However, as discussed above, the difference between the beam attenuation and light scattering estimates of PMC may be regarded as an index of large organic particles. For the deeper stations this beam attenuation excess, integrated over the upper 50 m water depth, again shows a decrease offshore and reveals a clear relationship to  $\tau^{\text{p}}$  (Fig. 3;  $r=-0.63$ ,  $n=13$ ,  $0.01 < P < 0.05$ ; excluding station V2200), which when compared with the excess beam attenuation/POC relationship (Fig. 3) suggests that as the overall particle concentration decreases offshore, finer more organic depleted particles become dominant and particle residence times increase.

A possible corollary of this relationship is that particulate export across this margin is mainly driven by larger organic rich particles, which must be faster sinking. Both regional and temporal changes in  $\text{POC}/^{234}\text{Th}$  ratio may occur as a function of local production and export balances (Buesseler *et al.* 1995).  $\text{POC}/^{234}\text{Th}$  across the Iberian margin range between 5 and 60  $\mu\text{mol dpm}^{-1}$  and show considerable variability. Nevertheless, in general highest values are seen on the shelf and a slight decreasing offshore trend is noted ( $R=0.54$ ;  $n=13$ ,  $P < 0.01$ ), with values at water column depths  $>1000$  m being typically below 25  $\mu\text{mol dpm}^{-1}$ . The elevated  $\text{POC}/^{234}\text{Th}$  ratios reported here are similar to the high values found (14-23  $\mu\text{mol dpm}^{-1}$ ) for 0.5-1  $\mu\text{m}$  particles during bloom conditions in the North Atlantic (Buesseler *et al.*, 1992). This may not be surprising, as the bloom conditions may be analogous to the higher productivity conditions on the shelf seen here. However, it should be noted that  $\text{POC}/^{234}\text{Th}$  ratios in sediment trap material (*i.e.*, large, sinking aggregates) are often considerably lower (2-10 x; Buesseler *et al.*, 1992; Moran *et al.*, 1997) and so our POC and PON export fluxes should be regarded as an upper estimate.

#### 2.3.2. Comparison with new production estimates

Primary production was measured by  $^{14}\text{C}$  incubations at nine stations during the *CDI05* cruise and ranged between 43 and 162  $\text{mmol-C m}^{-2} \text{d}^{-1}$  (Ian Joint and Andy Rees, *personal communication*). There is generally an offshore decrease with the lowest overall rate of carbon fixation found at the most southerly station on transect V. Estimates of nitrogen assimilation suggest that most of the nitrogen requirement of the phytoplankton was met by ammonium assimilation, suggesting regeneration processes were dominant during this period (Ian Joint and Andy Rees, *personal communication*).

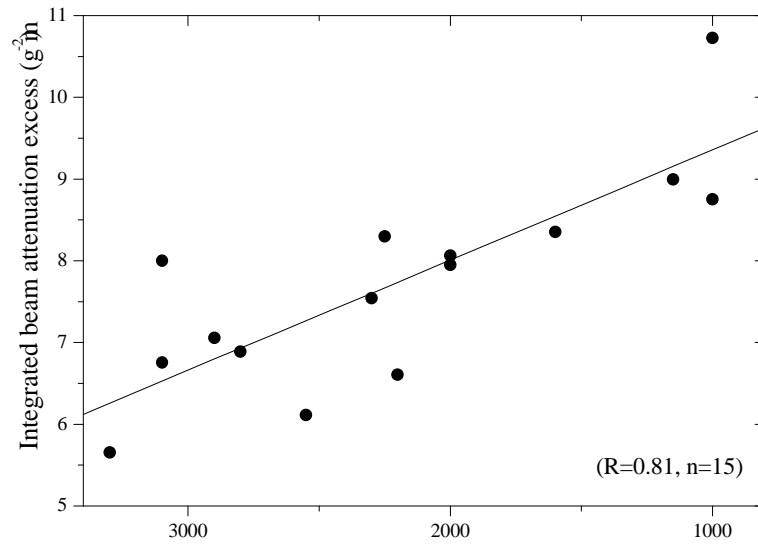


Fig. 3: The beam attenuation excess (as defined in Fig 2) particulate matter load integrated over the upper 50-m water depth for the offshore stations ( $\geq 1000$  m) against water column depth.

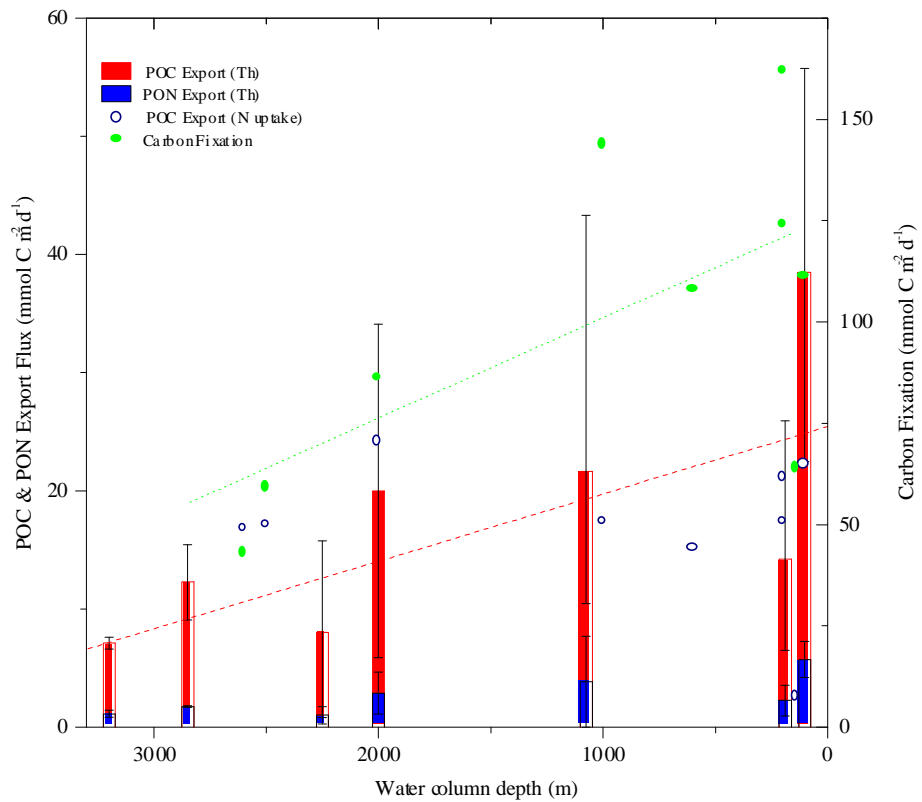


Fig. 4: Average POC and PON export flux estimates based on  $^{234}\text{Th}$  together with carbon fixation and POC export based on N uptake against water column depth. The bars represent the mean value of all station from similar depths north to south. The error bars give the range of all data from a given station depth.

Due to the high pressure on water collected during the cruise, the single station (N2000) where primary production and  $^{234}\text{Th}$  were measured, the ratio of POC export *versus* total production at this station was 28% based on new production estimates (*i.e.*, *f*-ratio; Ian Joint and Andy Rees, *personal communication*) and 39% based on the  $^{234}\text{Th}$  export flux. It is not necessary for export fluxes and new production based on nutrient uptake experiments to balance on short time scales (Buesseler *et al.*, 1992). However, a general comparison is presented in Fig. 4, showing average POC and PON export fluxes together with carbon fixation estimates for the northern Iberian Margin during the pre-upwelling period.

The constant  $^{234}\text{Th}$  export flux found across this margin contrasts with the decreasing offshore trend in the POC export flux apparent in Fig. 4, which is primarily supported by the variation seen in the POC/Th<sup>P</sup> ratio. This is consistent with the decreasing offshore trend in both carbon fixation and the apparent index of large organic particles present in the upper water column suggested by the optical properties. The trends apparent in Fig. 4 are likely to be more robust than any single measurement, with the ratio of the two slopes suggesting that an average of 19% of the primary production is lost as a sinking particulate flux.

Overall the pre-upwelling situation observed during *CD105* was characterised by low phytoplankton biomass, primary production based on ammonium regeneration and low POC export fluxes. Such conditions are likely to be considerably different during the summer upwelling season when the new source of nutrients induces a net increase in phytoplankton biomass.

### 3. SEDIMENTS

As outlined in the first annual report we have collected a total of 4 Kasten (See: Table 1, first annual report) and 7 box cores from the OMEX II-II Region. Our objectives during the second year of the programme have been two-fold: first, to develop age models for each of the cores and second, to determine the major and minor elemental concentration of the bulk sediment. The former is critical in our ability to calculate component fluxes (in particular organic carbon fluxes) which together with the latter objective will allow us to investigate the potential of reconstructing the history of upwelling and its effects on palaeoproductivity since the last glacial maximum.

#### 3.1. Age models

The age model for the OMEX Kasten cores are presently based upon features in the oxygen isotopic profiles, together deposits of the latest two ice-rafting pulses known as 'Heinrich events' (Heinrich, 1988; Broecker *et al.*, 1992). Oxygen isotope curves have been generated for core OMEX II-9K (Fig. 5) and OMEX II-5K and each show typical structure since the last glacial maximum. The final age models are presently under construction and involve the correlation (isotopes,  $\text{CaCO}_3$  and magnetic susceptibility records) with the high-resolution core MD95 2040 (see below).

It is necessary that AMS  $^{14}\text{C}$  dating be carried out on mono-specific foraminifera samples in order to provide detailed age constraints within the Holocene.

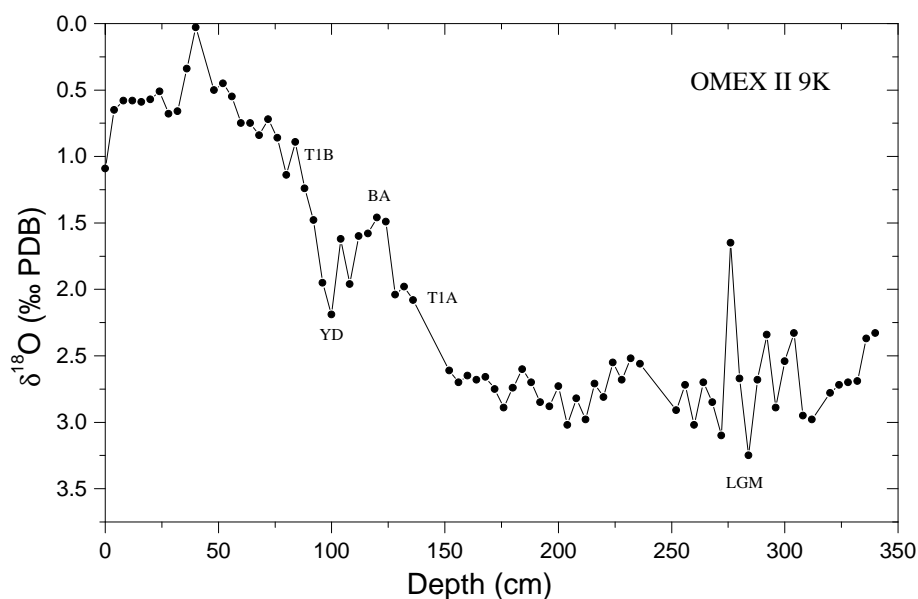


Fig. 5: Oxygen isotope curve for core OMEX II-9K. LGM= Last Glacial Maximum; T1A =Termination 1A; BA= Bølling allerød; YD= Younger Dryas and T1B= Termination 1B.

### 3.2. Palaeoproductivity

The elemental concentrations of Al, Ba, Ca, Cu, K, P, Si, Ti and V for each of the OMEX II-II cores (at 4 cm resolution) have been determined using a Perkin Elmer Plasma 40 ICP-AES. Sediment compositional variations have been monitored through normalisation of elemental concentrations by aluminium.

The apparent link between productivity and barite formation (François *et al.*, 1995) has lent support to the suggestion that Ba accumulation in deep marine sediment may be used for reconstructing palaeoproductivity (*e.g.*, Goldberg and Arrhenius, 1958; Schmitz, 1987; Dymond *et al.*, 1992; Shimmiel, 1992; Dymond and Collier, 1996; Thomson *et al.* in press). The method relies on the flux of biogenic Ba (bio-Ba), during periods of high productivity, becoming large enough for it to be readily identified against the detrital Ba present in aluminosilicates, measured within the total sediment (Ba/Al).

At present no quantitative relationship exists between bio-Ba and export productivity because the mechanisms by which the bio-Ba/Corg ratio is fixed during production and the alteration of the ratio as the particles sink through the water column are not well understood (François *et al.*, 1995; Dymond and Collier, 1996). It is evident from Fig. 6 (and other OMEX Kasten cores) that the concentration of organic carbon on the Iberian margin is low (typically < 0.5 % wt). This is reflected in the low Ba/Al ratios found for most of the record, which typically reflect detrital Ba. Nonetheless an interesting peak in both organic carbon and Ba is present during the mid-Holocene. This peak may correspond to the Holocene Climatic Optimum, but we await more detailed AMS dating to confirm the age of this peak. Recently Thomson *et al.* (in press) has shown simultaneous peaks in organic carbon, diatom abundance and Ba/Al occur at the isotope stage boundaries, in particular 10/9, 6/5 and 2/1, in core MD95-2036 located west of Oporto Seamount.

### 3.3. Micropalaeontology and Lithology

Core OMEX II-5K was chosen for inclusion in a Ph.D. study (L. de Abreu, University of Cambridge) investigating the palaeoecological and palaeoceanographic change on the Iberian Margin over the last glacial cycle. The study has employed a combination of information derived from the analysis of micropalaeontological, biostratigraphical and sedimentological data.

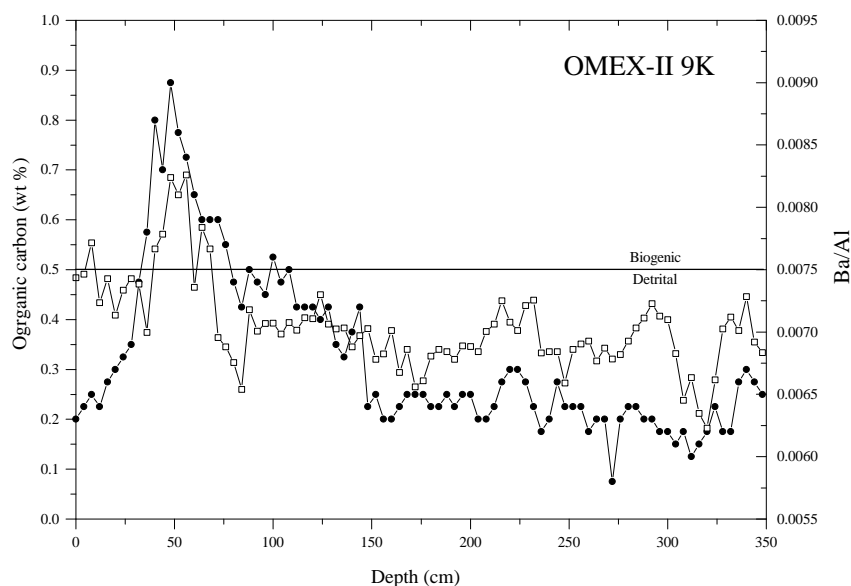


Fig. 6. Organic carbon and Ba/Al mass ratio against depth for OMEX II-9K.

A total of 25 different species of planktonic foraminifera were identified in the > 150  $\mu\text{m}$  fraction. All species belonged to living fauna and were grouped into five distinctive assemblages according to their ecological preferences. In the present day these assemblages are associated with distinct water masses.

As found in other cores on the Iberian Margin, OMEX II-5K contains distinct horizons with increased terrigenous material that are thought to correspond, at least in part to ice-rafting events. These horizons can be compared with Heinrich layers described in numerous studies for other sectors of the eastern North Atlantic (Bond, *et al.*, 1992, 1993; Manighetti *et al.*, 1995; Lebreiro *et al.* 1996). Lithological analysis shows quartz as the dominant component in these layers along with detrital carbonate, volcanics, mafic minerals, basalt lithoclasts and mica. Other lithics, derived from the nearby continental shelf, show up in significant amounts both within and outside Heinrich Layers.

Using the distribution of the planktonic foraminiferal microfauna, the relative abundance of species throughout the core has been compared with the position and mineralogical composition of the terrigenous levels. The coarse fraction lithic counts correlate fairly closely with the maximum abundance of the left coiling variety of *Neogloboquadrina pachyderma*. The presence of ice rafted detritus in association with these abundance peaks provides an additional argument for the influence of meltwater resulting from the fusion of migrating icebergs, that acted as the transport mechanisms for the terrigenous particles to lower latitudes.

The relation between microfaunal assemblages and sea surface temperature (SST) data was estimated using the modern analogue technique (Pflaumann *et al.*, 1996). As in other North Atlantic areas the strongest detrital peaks are associated with cooling phase maxima, followed by warming to almost interglacial temperatures. Foraminiferal census counts also imply a significant drop in the SST of 8-12°C during these events.

The potential for correlating OMEX II-5K with other high resolution records for the same region by aligning the microfaunal and sedimentological records is limited due to the low resolution, as well as lack of many distinctive features of this core. However, an age model is being developed by correlation with other more detailed records and with GISP2 ice core.

### 3.4. Sediment grain-size and palaeocurrent reconstruction

As part of our goal to examine the historical aspects of the sedimentary regime along the Iberian Margin, we have obtained samples originally collected as part of the International Marine Global Change Studies (IMAGES) programme. The samples from core MD95-2040, a 35 m *Calypso* giant piston core, were recovered from a location east of Oporto Seamount in a water depth of 2465 m



(Bassinot and Labeyrie, 1996). Using the ( $^{230}\text{Th}_{\text{excess}})_0$  method, Thomson *et al.* (1999) has examined the record of sediment accumulation in MD95-2040 occurring over the past 140,000 years, a period that includes the last two full glacial/interglacial transitions. This work has shown that pattern of sedimentation in the basin is related to both sea level control of the supply of terrigenous material and sediment redistribution and focusing (contourite formation). The latter appears too be particularly active during glacial times and may be a result of a systematic change in the deep ocean circulation in response to climate forcing. We have completed a detailed sedimentological analysis of this core, including determination of the sortable silt index for near bottom current speed. We are currently interpreting the results which appear to show the presence of a strong and coherent glacial/interglacial cyclicality in the near bottom current strength. This variability suggests enhanced depositional fluxes (mainly of fine material) occurs during periods of slow current speed (*i.e.*, allowing deposition) and presumably increased fine sediment supply, namely during glacial times.

### 3.5. Results of diatom analysis in surface and down-core sediments of the NW Iberian margin

The major role of the Universidade da Coruña is a) to establish by means of diatom analysis in bottom sediments the relationship between present day oceanographic conditions and the contemporary sedimentary record in across slope transects of the NW Iberian and b) to help in the reconstruction of the palaeoceanography of the region, back to the last glacial maximum, using down-core diatom assemblages mainly as indicators of upwelling, palaeoproductivity and freshwater influence. This report shows results on diatom distribution in surface sediment and piston core samples taken during the *Pelagia PE109* and *PE121* cruises.

Surface sediment samples were taken with a box-core following transects perpendicular to the margin during the *Pelagia PE109* and *PE121* cruises in 1997 and 1998 respectively. A 5.40-m long piston core (*PE109-13* pc, 42.20°N 9.41°W) was also sampled at 10 cm intervals. The upper 0.5-cm surface sediment of the box-cores was extracted for analysis. All the samples were treated following standard acid cleaning (Schrader, 1973) with some minor modifications. An aliquot of each cleaned sample was mounted on 22 x 22 mm coverglasses with Naphrax diatom mountant (refractive index = 1.7). Due to the scarcity of diatoms, the clean sample was concentrated in the slides as much as possible. Diatom counts were made at 1000 X magnification using a Nikon Eclipse 600 microscope with Nomarski differential contrast. A minimum of 200 valves were counted per sample. Absolute diatom concentrations were estimated adding exotic *Lycopodium* spores to the samples.

All the analysed samples showed a high degree of dissolution and/or fragmentation of the diatom valves. Deterioration made identification to the species level very problematic in some genus such as *Thalassiosira*. Diatom dissolution was extreme in the *PE109-13* piston core, which was absolutely barren of diatoms with the exception of the 150 to 90 cm stretch where some sparse diatom fragments were detected. Absence of diatoms at least in this core did not allow any diatom-based reconstruction of the upwelling history of the region. This result contrasts with previous diatom studies in southernmore positions where an almost continuous diatom record extended back to 100 ka (Abrantes, 1991).

Absolute diatom content and percent distribution of the most significant taxa in the surface sediments were determined (Fig. 7). Adverse preservation conditions made diatom counts impossible in some samples (circles not included in the grayed areas of Fig. 7). Diatom concentrations in the sediments (valves  $\text{g}^{-1}$ , Fig. 7) show high values compared to previous data on the Galician continental shelf (Bao *et al.*, 1997) and are typical of an area subjected to upwelling phenomena. There is a net offshore increase in diatom concentrations for the three selected transects perpendicular to the margin. However an important diminution occurs at the most oceanic station (*PE109-08*). Provisional estimates of diatom accumulation rates for samples taken during the *Pelagia* cruise of 1997 show no direct relationship with total mass fluxes.

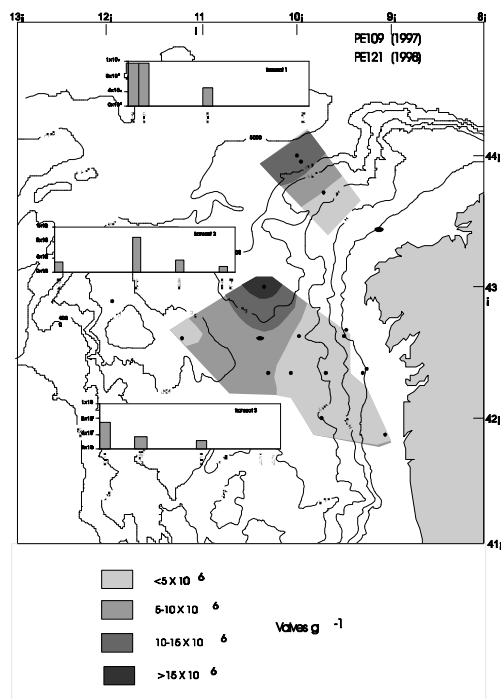


Fig. 7: Distribution of diatom valves per gram of dry sediment.

Diatom assemblages are mainly composed by *Chaetoceros* resting spores (Fig. 8). Their abundance in the sediments is related to areas of high productivity conditions. This taxon dominates all the stations with the exception of station *PE109-08*. The low percent abundance found at this station as well as of the total diatom concentration would probably indicate the limit where upwelling exerts a primary role in the composition of diatom assemblages preserved in the sedimentary cover. As for the Goban Spur margin, no taphonomical indications could be found in the state of preservation of the spores in order to dilucidate the contribution of shelf-derived *Chaetoceros* to the sediments.

The genus *Thalassiosira* has been reported as one of the main components of diatom assemblages in the Galician and Portuguese diatom taphocoenoses, being related to areas where nutrient supply would be more consistent and avoiding areas with a more pulse-like nutrient supply situation (Abrantes, 1988; Bao *et al.*, 1997). Maximum relative abundances are found in the NW corner of the study area coinciding with areas of maximum diatom content in valves  $g^{-1}$  (Fig. 9). In contrast with the Galician shelf, there is no relationship between a high productivity indicator such as the *Chaetoceros* resting spores relative abundances and diatom concentrations ( $r=0.38$ ,  $p>0.05$ ). However this correlation is found between the later and *Thalassiosira* spp. percent abundances ( $r=0.69$ ,  $p<0.01$ ). According to the known *Thalassiosira* autoecology, surface sediment diatom enrichment in the area could be more related not to pulse-like upwelling situations but to processes operating in a way that would give a more consistent nutrient supply to the water column. This interoperation assumes that in the Galician margin, due to the weaker character of the BNL, diatom assemblages reflect more closely the characteristics of the overlying water column than in Goban Spur where diatom taphocoenoses were probably more affected by shelf-derived allochthonous enrichment.

The minimum amount of displaced diatoms reaching the slope seafloor can be estimated on the basis of the distribution of tychoipelagic and benthic diatoms, taxa restricted to live in the inner shelf. Maximum relative abundance for the sum of both groups is recorded at the upper slope station *PE109-13* where at least 18% of the total diatom assemblage is composed by diatoms displaced from shelf positions. This figure coincides with similar values found in Goban Spur.

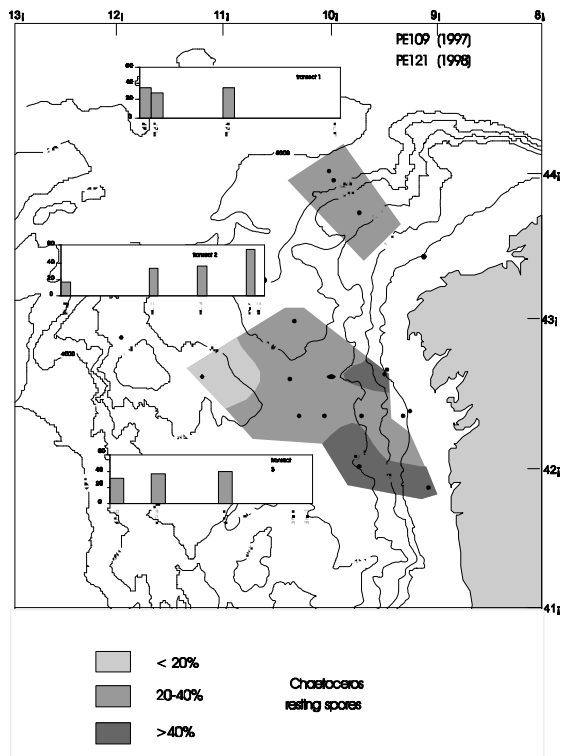


Fig. 8: Relative abundance of *Chaetoceros* spp. resting spores.

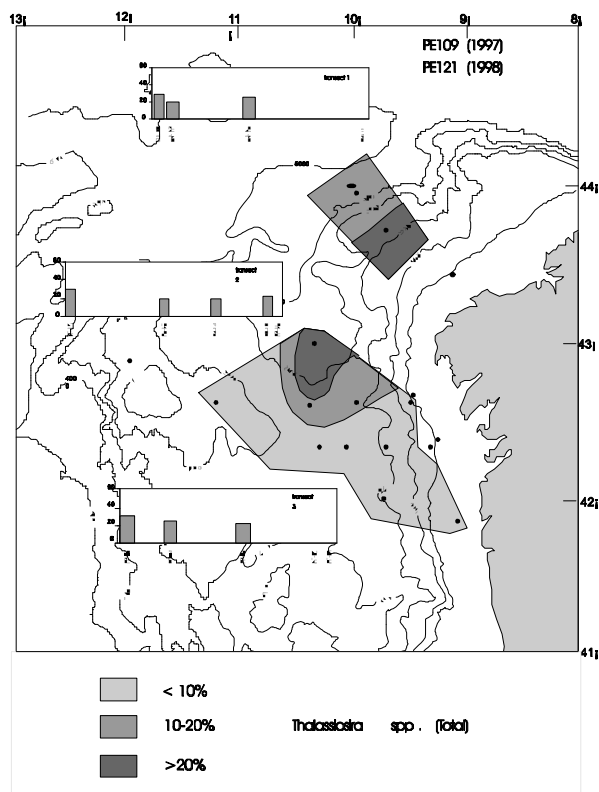


Fig. 9: Relative abundance of *Thalassiosira* spp.

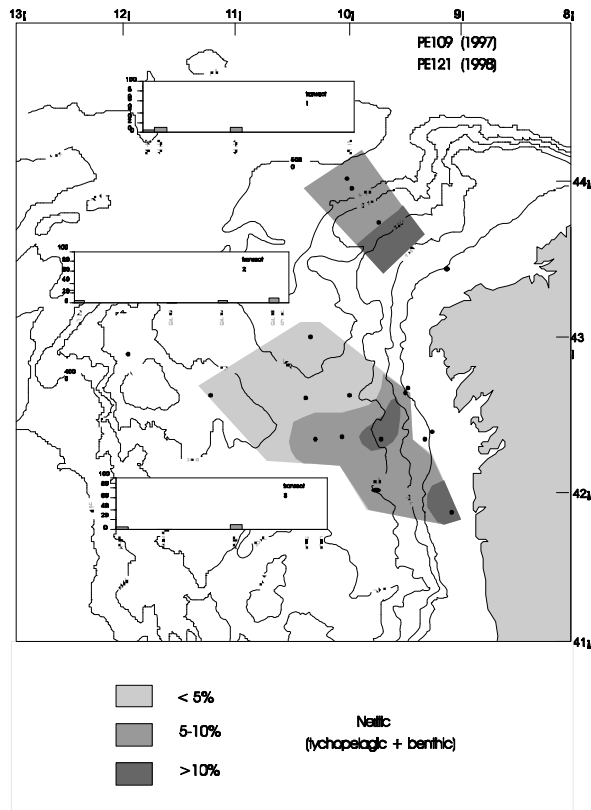


Fig. 10: Relative abundance of tychopelagic plus benthic diatoms.

## REFERENCES

- Abrantes F. (1988) Diatom assemblages as upwelling indicators in surface sediments off Portugal. *Marine Geology*, 85, 15-39.
- Abrantes F. (1991) Increased upwelling off Portugal during the last glaciation: diatom evidence. *Marine Micropaleontology*, 17, 285-310.
- Baskaran M., Santschi P.H., Guo L., Bianchi T.S. and Lambert C. (1996)  $^{234}\text{Th}$ : $^{238}\text{U}$  disequilibria in the Gulf of Mexico: the importance of organic matter and particle concentration. *Continental Shelf Research*, 16, 353-380.
- Bishop J.K.B. (1999) Transmissometer measurement of POC. *Deep Sea Research*, 46, 353-369.
- Bao R., Varela M. and Prego R. (1997) Mesoscale distribution patterns of diatoms in surface sediments as tracers of coastal upwelling of the Galician shelf (NW Iberian Peninsula). *Marine Geology*, 144, 117-130.
- Bassinot F. and Labeyrie L. (1996) Images MD 101 à bord du Marion Dufresne du 29 mai au 11 juillet 1995. *Publication de l'Institut Français pour la Recherche et la Technologie Polaires*, No. 96-1 (1996)
- Bond G., Heinrich H., Broecker W., Labeyrie L., McManus J., Andrews J., Huon S., Jantschick R., Clasen S., Simet C., Tedesco K., Klas M., Bonani G. and Ivy S. (1992). Evidence for massive discharges of icebergs into the North Atlantic Ocean during the last glacial period. *Nature*, 360, 245-249.
- Bond G., Broecker W., Johnsen S., McManus J., Labeyrie L., Jouzel J. and Bonani G. (1993) Correlations between climate records from North Atlantic sediments and Greenland ice. *Nature*, 365, 143-147.
- Broecker W., Bond G., Klas M., Clark E. and McManus J. (1992) Origin of the northern Atlantic's Heinrich events. *Climate Dynamics*, 6, 265-273.
- Buesseler K.O., Bacon M.P. Cochran J.K. and Livingston H.D. (1992) Carbon and nitrogen export during the JGOFS North Atlantic Bloom Experiment estimated from Th-234/U-238 disequilibria. *Deep-Sea Research*, 39, 1115-1137.
- Buesseler K.O., Andrews J.A, Hartman M.C. Belostock R. and Chai F. (1995) Regional estimates of the export flux of particulate organic carbon derived from thorium-234 during the JGOFS EqPac program. *Deep-Sea Research II*, 42, 777-804.
- Dickson R.R. and McCave I.N. (1986) Nepheloid layers on the continental slope west of Porcupine Bank. *Deep-Sea Research*, 33, 791-818.
- Gardner W.D., Walsh I.D. and Richardson M.J. (1993) Biophysical forcing of particle production and distribution during a spring bloom in the North Atlantic. *Deep-Sea Research*, 40, 171-195.
- Goldberg E.D. and Arrhenius G.O.S. (1958) Chemistry of pelagic Pacific sediments. *Geochimica et Cosmochimica Acta*, 13, 153-212.
- François R., Honjo S., Manganini S.J. and Ravizza G.E. (1995) Biogenic barium fluxes to the deep sea: Implications for paleoproductivity reconstruction. *Global Biogeochemical Cycles*, 9, 289-303.
- Gross T.F.R. and Williams A.J. (1991) Characterisation of deep sea storms. *Marine Geology*, 99, 281-301.
- Heinrich H. (1988) Origin and consequences of cyclic ice rafting in the northeast Atlantic Ocean during the past 130,000 years. *Quaternary Research*, 29, 143-152.
- Lebreiro S.M., Moreno J.C., McCave I.N. and Weaver P.E.E. (1996) Evidence for Heinrich Layers off Portugal (Tore Seamount: 39°N, 12°W. *Mar. Geol.* 131, 47-56.
- Martin J.H., Fitzwater S.E., Gordon R.M., Hunter C.N. and Tanner S.J. (1993) Iron, primary production and flux studies during the JGOFS North Atlantic Bloom Experiment. *Deep-Sea Research*, 40, 115-134.
- Niven S.E.H., Kepkay P.E. and Boraie A. (1995) Colloidal organic carbon and colloidal  $^{234}\text{Th}$  dynamics during a coastal phytoplankton bloom. *Deep-Sea Research*, 42, 257-273.
- Moran S. B., Ellis K.M. and Smith J.N. (1997)  $^{243}\text{Th}$ / $^{238}\text{U}$  disequilibrium in the central Arctic Ocean: implications for particulate organic carbon export. *Deep Sea Research II*, 44, 1593-1606.

- Santschi P. H. and Honeyman B. D. (1991) Radioisotopes as tracers for interactions between trace elements, colloids and particles in natural waters. In: *Heavy metals in the Environment*. Vernet J.-P. ed. (Elsevier, Amsterdam), pp. 229-246.
- Schmitz B. (1987) Barium, equatorial high productivity, and the northward wandering of the Indian Continent. *Palaeoceanography*, 2, 63-77.
- Schimmield G.B. (1992) Can sediment geochemistry record changes in coastal upwelling palaeoproductivity? Evidence from northwest Africa and the Arabian Sea. In: *Evolution of Upwelling Systems Since the Early Miocene*, edited by E.P. Summerhayes *et al.*, *Geol. Soc. Spec. Publ. London*, 64, 29-46.
- Dymond J., and Collier R. (1996) Particulate Barium fluxes and their relationship to biological productivity. *Deep-Sea Research II*, 43, 1283-1308.
- Dymond J., Suess E. and Lyle M. (1992) Barium in the deep-sea sediments: A geochemical proxy for paleoproductivity. *Paleoceanography*, 7, 163-181.
- Manighetti B. and McCave I.N. (1995a) Depositional fluxes paleoproductivity and ice-rafting in the northeast Atlantic over the past 30ka. *Paleoceanography*, 10, 657-667
- McCave I.N. (1984) Erosion, transport and deposition of fine-grained marine sediments. In: *Fine-Grained Sediments: Deep Water Processes and Facies*. Geological Society of London Special Publication, 15, 35-69.
- Rudniki M. D. (1997) A computer program for plotting oceanographic fence diagrams. *Computers and Geosciences*, 23, 209-213.
- Schrader H. J. (1973) Proposal for a standardized method of cleaning diatom-bearing deep-sea and land-exposed marine sediments. *Nova Hedwigia, Beihefte*, 45, 403-409.
- Thomson J. Nixon S., Summerhayes C.P., Schonfeld J., Zahn R. and Grootes P. (1999) Implications for sedimentation changes on the Iberian margin over the last two glacial/interglacial transitions from ( $^{230}\text{Th}_{\text{excess}}\text{)}_0$  systematics. *Earth and Planetary Science Letters*, 165, 255-270.
- Thomson J. Nixon S., Summerhayes C.P., Rohling E.J., Schonfeld J., Zahn R., Grootes P., Abrantes F., Gasper L. and Vaqueiro S. (in press) Enhanced productivity on the Iberian Margin during glacial/interglacial transitions revealed by barium and diatoms.
- Thorpe S.A. and White M. (1988) An intermediate nepheloid layer. *Deep-Sea Research*, 35, 1655-1671.